Journal of Microscopy, Vol. 198, Pt 1, April 2000, pp. 1–9.
Received 15 March 1999; accepted 29 November 1999

Images of absolute retardance $L \cdot \Delta n$, using the rotating polariser method

M. A. GEDAY, W. KAMINSKY, J. G. LEWIS & A. M. GLAZER
Clarendon Laboratory, Department of Physics, University of Oxford, Parks Road, Oxford OX1 3PU, U.K.

Key words. Absolute double refraction, birefringence, fringe order, indicatrix, interferometry, light microscopy, polarized light.

Summary

Modulation techniques for measuring changes in optical birefringence, such as the rotating-polariser method (Wood & Glazer, 1980, *J. Appl. Crystallogr.* **13,** 217), allow one to determine $|\sin \delta|$, $\delta = 2\pi L\Delta n/\lambda$, Δn = double refraction, L = light path and λ = wavelength. However, they generally suffer from not providing absolute values of the optical retardance or are limited to relatively low retardance values. In addition, knowledge of the absolute phase is required when establishing the correct values of optical orientation information. In this paper, it is shown how the phase δ, and thus optical retardance, can be extracted from combining measurements of $|\sin \delta|$ at different wavelengths. The new approach works on each single point of a 2-D picture without the need to correlate with neighbouring points. There is virtually no limit to the retardance, and the computational efforts are small compared with other methods (e.g. Ajovalasit *et al.* 1998, *J. Strain Analysis* **33**, 75). When used with imaging techniques, such as the rotating polariser method of Glazer, Lewis & Kaminsky 1996 (*Proc. R. Soc. London Series* **A452**, 2751) this process has the potential to identify automatically optically anisotropic substances under the microscope. The algorithm derived in this paper is valid not only for birefringence studies, but can be applied to all studies of interfering light waves.

1. Introduction

It is well known that polarized light is commonly used to determine the double refraction of an optically anisotropic material such as a crystal, organic tissues, strained glasses, polymers, etc. Double refraction, also known as plano-birefringence (Shurcliff, 1962), is given by $\Delta n = (n_2 - n_1)$, where n_1 and n_2 are the refractive indices corresponding to the cross-section of the optical indicatrix seen down the viewing direction (Fig. 1a) (Hartshorne & Stuart, 1964). Traditionally, this has been measured using a variety of crystal compensator techniques. However, in recent times, the availability of imaging systems and computers has led to many different attempts to derive the double refraction automatically with high resolution at different locations within an image of the specimen (e.g. Ajovalasit *et al.*, 1998).

Automated optical measurement techniques are important in many different research fields, e.g. the study of phase transitions, measurements of photoelasticity, and in biology. In the study of phase transitions it is necessary to measure accurately how the optical retardance (or retardation) changes with temperature and to observe the formation of domain structure. In photoelasticity experiments, the measurement of strain-induced double refraction in, for example, constructional materials, is used to assess the location and magnitude of applied stresses. Determination of the double refraction in biological samples is of value for structural studies (Whittaker, 1995).

The direct measurement of double refraction in an image of the specimen involves accurate measurements of intensity. Calculation of the double refraction from this intensity then involves the evaluation of trigonometric functions with phase δ as an argument.

$$\delta = L(n_2 - n_1)k \tag{1}$$

where $k = 2\pi/\lambda$ is the length of the wave vector of the light, L is the sample thickness and δ is the phase difference between the two eigenmodes of the light. The product of the light path, L, and double refraction $(n_2 - n_1)$, is the retardance, Γ. The number of multiples of 2π in the arguments of these trigonometric functions, which we call the order (the number of multiples of π is in the field of photoelastics known as the fringe-order), cannot be derived from the trigonometric functions alone, as these are periodic, and so

Correspondence to: Professor M. Glazer. Tel: + 44 (0)1865 272334; fax: + 44 (0)1865 272400; e-mail: glazer@physics.oxford.ac.uk

© 2000 The Royal Microscopical Society

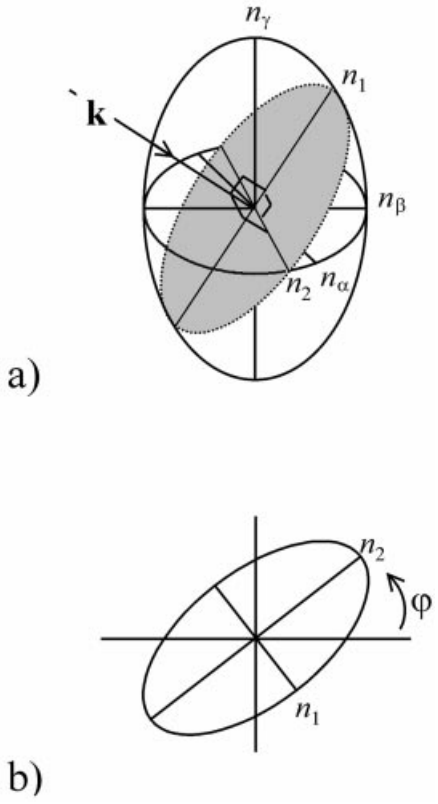

Fig. 1. The indicatrix. (a) A general indicatrix with the three major refractive indices n_α, n_β and n_χ. The incoming light, described by the wave vector **k**, will experience a double refraction $(n_2 - n_1)$, where n_1 and n_2 are expressed in the lengths of the semi-axes of the ellipsoidal cross-section of the indicatrix perpendicular to **k**. (b) The definition of extinction angle φ used in the text. Polarization of light parallel to the larger n_2 corresponds to slower propagation of the wave.

this introduces an ambiguity. Thus, in general, the double refraction cannot be accessed directly by image analysis, and additional measurements are necessary to solve the order ambiguity.

As a first step, the value of the trigonometric functions is determined and the eigenmode directions of the refractive indices n_1 and n_2 are separated out by deriving the extinction angle φ (Fig. 1b) between the modes and a reference system. The order ambiguity is usually removed in a second step. A number of methods associated with step one are given by Ajovalasit *et al.* (1998). Step two can also be carried out in various ways. It is known from basic polarization microscopy that information about the order is contained in the colours which are seen when a specimen is viewed such that $\varphi = 45°$ between crossed polars in white light (e.g. Hartshorne & Stuart, 1964). The so-called Michel–Levi chart maps the colours against the retardance, and for a known thickness, the double refraction can be read out. This can often be used as a fingerprint for different rock-minerals. However, the colours vary between different materials and depend on the spectral composition of the light source. One normally has to rely on ordinary compensator methods to find the absolute value of the retardance, in which case it is necessary to rotate the sample in order to adjust the extinction angle for each region of the sample. This is clearly not suitable for an imaging system in which there may be a multitude of different regions in the field of view with different optical orientations.

A computerized measurement could quantify the colour-equivalent of the Michel–Levi chart, using any of the methods of step one, and compare it with a calibration in the same material. This approach is called the RGB-method, as it involves the red, green and blue values of a video camera with which the experiment is made (Ajovalasit *et al.*, 1995).

Another approach involves the measurement of the spectral dependence of a small sample region, employing a monochromator to allow for several individual measurements with respect to wavelength. This method is called spectral contents analysis (SCA) (Redner, 1985).

The order is accessed from the change in lateral positions of minimum intensity for two different wavelengths in a crossed-polars experiment, where the intensity of the transmitted light when $\varphi = 45°$ is given by

$$I = I_0 \sin^2(\delta/2) \qquad (2)$$

Here I_0 is the initial light intensity. This requires a 2-D image of the sample measured at least twice, one for each wavelength. The images are compared laterally to enumerate the fringes. Three wavelengths have been used to produce absolute retardance and extinction, provided that there exists a region with zero retardance within the sample where the images for different wavelengths are coincident (Buckberry & Towers, 1996).

Determining the absolute order is particularly important when working on systems undergoing changes because, for instance, an increase in $|\sin\delta|$, which is what is generally measured, does not, in general, correlate with an increase in δ. Furthermore, knowledge of the order makes it possible to consistently assign the extinction angle φ to the slow axis of the indicatrix, which is a shortcoming of all automated methods.

The aim of the present paper is to show how to remove the ambiguity when measuring the retardance Γ on a single point, using the so-called rotating polariser (RP) method in which measurements of $|\sin\delta|$ can be made with ease, and employing only a maximum of three close wavelengths when the intrinsic optical dispersion of the retardance is small. We shall show that, with a small amount of computational effort, quite large δ-values in a variety of samples can be calculated with high accuracy.

The approach used here has analogy with phase stepping interferometry (see Greivenkamp & Bruning, 1992).

2. Theory

2.1. Methods to measure the retardance and extinction angle

For a transparent birefringent sample which has been aligned between crossed polarisers the extinction angle φ normally refers to a reference system, usually measured anticlockwise between the horizontal axis and one of the eigenmode directions (see below and Fig. 1b). By varying either the sample orientation or the angles of the polarisers with respect to each other, one can derive the optical retardance (see for example Moxon & Renshaw, 1990). Similarly, a sample could be placed between a set of two circular polarisers made from a combination of a pair of crossed polarisers and a pair of crossed quarter-wave plates at 45° to the polarisers.

A different approach is to place the sample after a circular polariser, where the extinction does not matter and thus, the sample does not need to be aligned with the polarisers. The optical properties can be analysed with an ordinary polariser, which is then rotated. If the polariser is rotated continuously, the intensity of the light varies periodically. The phase shift of the signal contains the information on the extinction angle φ. The amplitude at an angular frequency 2ω, with which the polariser is rotating, is related to the retardance according to the following expression (t is the time):

$$I = \frac{I_0}{2}[1 + \sin 2(\omega t - \varphi)\sin\delta] \tag{3}$$

It is possible then to extract the term $|\sin\delta|$ from this intensity by Fourier analysis on 2ω using a lock-in amplifier and monochromatic light (RP-method, Wood & Glazer, 1980). This optical train can be classified as a semicircular polariscope. Equation (3) can also be evaluated through numerical Fourier analysis. To do this it is convenient to replace the continuous motion of the polariser by a stepper motor-driven polarization. In our system we have inverted the light path[1] (Fig. 2). This set-up resembles the phase-stepping method of Ajovalasit *et al.* (1998), although the optical train is different.

When rotating the polariser through a total of $\alpha_{\max} = 180°$ in N steps of $\alpha_i = \alpha_{\max}/N$, the intensity at the detector is still described by Eq. (3), which can be recast in the form below:

$$\begin{aligned} I_i &= a_0 + a_1 \sin 2\alpha_i + a_2 \cos 2\alpha_i; \\ a_0 &= \tfrac{1}{2} I_0, a_1 = \tfrac{1}{2} I_0 \sin\delta\cos 2\varphi, \\ a_2 &= -\tfrac{1}{2} I_0 \sin\delta \sin 2\varphi \end{aligned} \tag{4}$$

The parameters a_i are found from

$$a_0 = \sum_{i=1}^{N} \frac{1}{N} I_i,\ a_1 = \sum_{i=1}^{N} \frac{2}{N} I_i \sin\alpha_i,\ a_2 = \sum_{i=1}^{N} \frac{2}{N} I_i \cos\alpha_i \tag{5}$$

which is different from expressions used in ordinary phase-stepping methods (see for example Hecker & Morche, 1986).

[1]For most of the materials to be investigated it does not matter if the path of the light is inverted (with the exception of magnetic samples). Thus, in our set-up we place the rotating polariser below the sample.

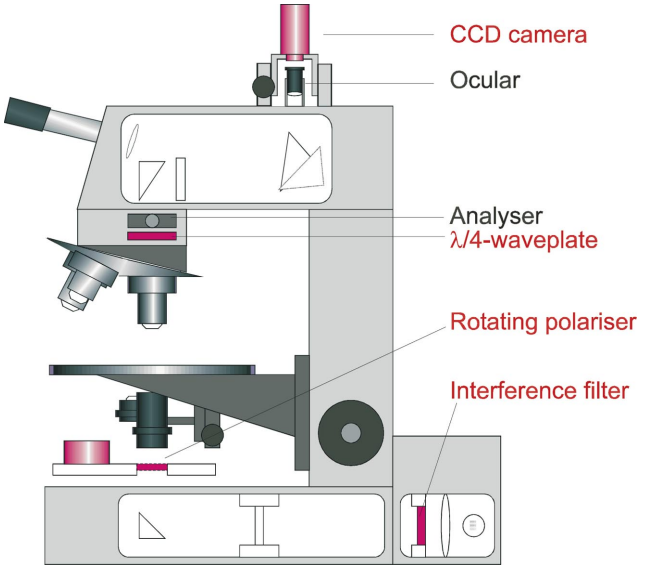

Fig. 2. The optical train as implemented on a standard polarizing microscope. The additional components of the rotating polariser method are highlighted in red.

The RP method has recently been developed further to produce false-colour microscope images of a sample with respect to three different features of the sample: the transmission $2I/I_0$, the sine (between 0 and 1) of the phase factor δ, i.e. $|\sin\delta|$, and the extinction angle φ (Glazer *et al.*, 1996). φ is calculated as $\varphi = 1/2 \arccos(a_1/\sqrt{a_1^2 + a_2^2})$.

It is of vital interest to consider Eq. (3) in more detail, by extending it to the case of a nonperfect quarter-wave plate and allowing for a varying initial intensity when the polariser is rotated. The resulting intensity can be calculated using Jones-matrices (see for example Hecht & Zajac, 1974). The initial amplitude E_0 changes by a percentage P with rotation angle α and offset α_0 according to

$$E_0 = E_0'(1 - P\cos(\alpha - \alpha_0)) \tag{6}$$

where E_0' is the amplitude of the light source. P is found by removing all the polarizing optical components with the exception of the rotating polariser itself. The experimental value of P is then used to correct all following intensity readings, which are divided by $(1 - P\ \cos(\alpha - \alpha_0))$. The extinction angle of the sample is denoted by φ and the quarter-wave plate (Fig. 2), mounted at 45° to the analyser, deviates from $\delta = \pi/2$ by a small amount, x:

$$\begin{aligned} \begin{pmatrix} E_x \\ E_y \end{pmatrix} = \frac{1}{2} &\begin{bmatrix} 1 & 1 \\ 1 & 1 \end{bmatrix} \begin{bmatrix} 1 & 0 \\ 0 & i - x \end{bmatrix} \begin{bmatrix} \cos\varphi & \sin\varphi \\ -\sin\varphi & \cos\varphi \end{bmatrix} \\ &\times \begin{bmatrix} \exp\frac{i\delta}{2} & 0 \\ 0 & \exp -\frac{i\delta}{2} \end{bmatrix} \begin{bmatrix} \cos\varphi & -\sin\varphi \\ \sin\varphi & \cos\varphi \end{bmatrix} \\ &\times \begin{bmatrix} \cos\alpha & -\sin\alpha \\ \sin\alpha & \sin\alpha \end{bmatrix} \begin{pmatrix} E_0 \\ 0 \end{pmatrix} \end{aligned} \tag{7}$$

The first vector at the far right of Eq. (7) represents the initial light amplitude. The matrices, from right to left, represent: the rotating polariser, the rotation of the sample by the extinction angle, the retardance of the sample, the transposed extinction-rotation, the quarter-wave plate, and the analyser at 45°. The final intensity is obtained from the light amplitude $\mathbf{E}=(E_x,\ E_y)$ as $I=\mathbf{E}\cdot\mathbf{E}^*$, where $\mathbf{E}^*$ is the complex conjugate of the amplitude **E**. The final result was obtained using the mathematical program MAPLE (Waterloo Maple Inc., 1996, website: http://www.maplesoft.com). With $I_0=E_0{}^2$ and neglecting terms in x^2 we find:

$$\frac{2I}{I_0}\cong 1+\sin 2(\alpha-\varphi)\cos\delta + x\left(\sin 2(\alpha+2\varphi)\sin^2\frac{\delta}{2}-\sin 2\alpha\cos^2\frac{\delta}{2}\right) \quad (8)$$

If the sample is removed ($\delta=0$), the effect of the quarter-wave plate is given by the last term, $x\sin(2\alpha)$ by which the light intensity is modulated. In practice, we have found typical values for x (after adjusting accurately to 45° towards the analyser) to be within 2% of the total intensity. The effect due to P is larger and ranges up to 10% in an ordinary microscope. The parameters a_1 and a_2 in Eq. (4) are changed to:

$$a_1=\frac{1}{2}I_0\left[\sin\delta\cos 2\varphi+x\left(\sin^2\frac{\delta}{2}\cos 4\varphi+\cos^2\frac{\delta}{2}\right)\right]$$
$$a_2=\frac{1}{2}I_0\left[-\sin\delta\sin 2\varphi+x\sin^2\frac{\delta}{2}\sin 4\varphi\right] \quad (9)$$

To achieve the highest accuracy, the necessary x-correction in Eq. (9) is carried out iteratively, using the parameters of Eq. (4) as starting values. However, this is only necessary when using optical components of poor quality. In the measurements presented here, using a high-quality quarter-wave plate and polarisers, the x-correction would not improve the results significantly.

Although the rotating-polariser plus CCD-imaging approach has already been used for a large variety of scientific problems and has proved to be very accurate, the magnitude of the retardance, as mentioned above, is only found as $|\sin\delta|$, and this means that the order is not obtained. To go further, one needs to find the absolute value of the phase δ. This can be done in principle by repeating the measurement with two or more close wavelengths.

In the following section it is shown how the absolute retardance is found without any further adjustment of the

Table 1. The assignment of the slope, Q, S_1, and S_2 as used in the programme to calculate δ. y_j symbolizes the $|\sin\delta|$ measured at wavelength j. η is a factor used to distinguish whether the two δs compared belong to the same half-order m. The table shows which y_j should be used for the $\delta_{0,1}$ and $\delta_{0,2}$ calculations and the value of the associated slope, Q, S_1, and S_2. The results originate from an analysis of possible relationships between the measured extinction angle φ_j and y_j, where it is assumed that $\lambda_1<\lambda_2<\lambda_3$ (i.e. $k_1>k_2>k_3$). This approach is not applicable for $Q>1$. If it is anticipated that Q will exceed 1 then a set of wavelengths closer together should be chosen. Where the slope is not shown, it has not been used in the calculations. In the algorithm used, the orientations are compared first; thereafter the magnitudes of $|\sin\delta|$ are compared. The procedure is found to work well when we take the value of η to be 0.95.

	$y_1\le y_2\ge y_3$	$y_1>y_3$ & not $y_1\le y_2\ge y_3$	$y_1<y_3$ & not $y_1\le y_2\ge y_3$
$\varphi_1=\varphi_2=\varphi_3$	$(y_1,\ y_3),\ S_1=-1,\ S_2=1,\ Q=1$	$(y_2,\ y_3),\ S_1=1,\ S_2=1,\ Q=0$ Slope >0	$(y_1,\ y_2),\ S_1=-1,\ S_2=-1,\ Q=0$ Slope <0
$\varphi_1=\varphi_2$ $\varphi_3=\varphi_1\pm 90$	$y_2<\eta y_1$	$y_2\ge\eta y_1$	
	$(y_2,\ y_3),\ S_1=1,\ S_2=-1,\ Q=0$ Slope >0	$(y_1,\ y_3),\ S_1=-1,\ S_2=-1,\ Q=1$ Slope >0	
$\varphi_1=\varphi_2\pm 90$ $\varphi_2=\varphi_3$	$y_2<\eta y_3$	$y_2\ge\eta y_3$	
	$(y_1,\ y_2),\ S_1=1,\ S_2=-1,\ Q=0$ Slope <0	$(y_1,\ y_3),\ S_1=1,\ S_2=1,\ Q=1$ Slope <0	
$\varphi_2=\varphi_1\pm 90$ $\varphi_1=\varphi_3$	$(y_1,\ y_3),\ S_1=1,\ S_2=-1,\ Q=1$		

sample. The improved RP method with shifted wavelength (SWRP-method) will then be applied to a variety of specimens to demonstrate its applicability.

2.2. Method to remove the ambiguity in the retardance

The ambiguity in determining the absolute phase (from measured $|\sin\delta|$ values, as derived with the RP method, is that $m\pi$, m an integer, can be added to the relative phase δ_0 without change of $|\sin\delta|$, where $2m$ is the order of the phase.

$$\delta = m\pi \pm \delta_0; \delta_0 = \sin^{-1}(|\sin\delta|). \tag{10}$$

The ambiguity may be solved from the derivative of the relative phase δ_0 with respect to the wavelength, which is expressed more conveniently using the wave-vector length, $k = 2\pi/\lambda$:

$$\frac{\partial\delta_0}{\partial k} = \pm\frac{\partial}{\partial k}(kL(n_2 - n_1) - m\pi)$$
$$= \pm L\left\{(n_2 - n_1) + k\frac{\partial}{\partial k}(n_2 - n_1)\right\}. \tag{11}$$

The second term in Eq. (11) describes the dispersion of the double refraction. If we assume that the effect of dispersion is small and can be neglected, recasting of Eq. (11) leads to:

$$\delta_1 = \pm k_1\frac{\partial\delta_0}{\partial k} = k_1\lim_{k_2\to k_1}\left(\frac{\delta_{0,2} - \delta_{0,1}}{k_2 - k_1}\right) \tag{12}$$

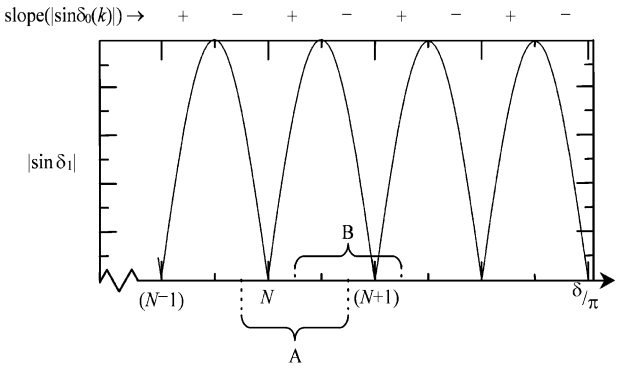

Fig. 3. Illustration of how the calculation of the order of δ is performed. The sign of the calculated slope of $|\sin\delta_0(k)|$ determines whether $\delta_1 \in [m\pi;\ m\pi + \pi/2]$ or $\delta_1 \in [m\pi + \pi/2;\ (m+1)\pi/2]$. This means that in the case of a positive slope any δ_1 calculated to be within the area $A = [m\pi - \pi/4;\ m\pi + 3\pi/4]$ will be assigned to the region $[m\pi;\ m\pi + \pi/2]$. Similarly, if the slope is negative and δ_1 is calculated to belong to B then it will be assigned to the region $[m\pi + \pi/2;\ (m+1)\pi/2]$. By finding m the ambiguity of the order is solved. The slope of $|\sin\delta_0(k)|$ follows the slope of $|\sin\delta_1|$ as the change in wavelength is reflected in a change in $\delta \propto k$. This is illustrated in Fig. 4, by the alternating sign in the difference between the measured $|\sin\delta_0|$ values.

$\delta_{0,1}$ and $\delta_{0,2}$ are the values of the relative retardance measured at two wavelengths 1 and 2 as defined in Eq. (10), and δ_1 is the calculated phase at the first chosen wavelength (the second chosen wavelength could just as well have been used for the δ calculations). When using measured data to calculate the absolute phase δ_1 we cannot simply use Eq. (12) because $\delta_{0,1}$ and $\delta_{0,2}$ (measured for different k_1 and k_2) might not belong to the same order of $\pi/2$. To take this possibility into account we must recast Eq. (12):

$$\delta_1 = \frac{k_1}{k_2 - k_1}(S_2\delta_{0,2} - S_1\delta_{0,1} - Q\pi) \tag{13}$$

Here S_1 and S_2 can take the values 1 and -1, depending on whether the ambiguous sign in Eq. (10) is positive or negative for $\delta_{0,1}$ and $\delta_{0,2}$. Q is the difference between the values of m of $\delta_{0,1}$ and $\delta_{0,2}$. Using an additional third wavelength we are generally able to find a pair of δ_0s to which we can assign appropriate S_1, S_2 and Q to calculate their difference correctly, as can be seen in Table 1. Note that the scheme in this table is applicable only when the change in wavelength results in a change in m less than 2 (although Eq. (13) is generally true). Thus, in order to use Table 1 one has to choose wavelengths sufficiently close to avoid a larger change in m.

The above δ calculations give roughly the correct value of the magnitude of δ, and thus the order. To solve the sign ambiguity in Eq. (10) it is useful to include information about the slope of $|\sin\delta_0(k)|$ at the wavelength used for the δ-calculations. The sign of the slope alternates with a period of $\pi/2$ in δ, as can be seen in Fig. 3, as does the sign in Eq. (10). Thus if, for example, the slope has been determined to be positive (using the analysis sketched in Table 1) then in general the final $\delta = m'\pi + \delta_0$, where m' is the fringe order calculated from the above δ calculations. Occasionally, though, the initially calculated δ is actually closer to $(m'+1)\pi + \delta_0$. In this case we reassign the fringe order

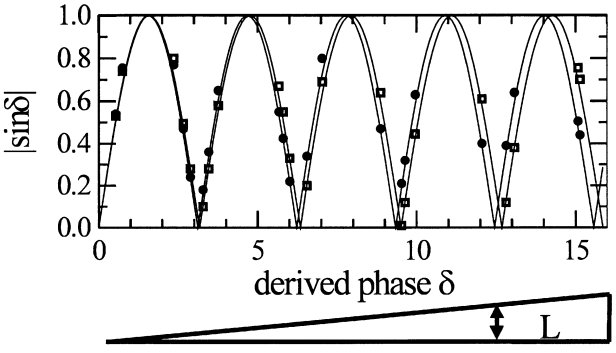

Fig. 4. Measured pairs of $|\sin\delta|$ for 540 nm (●) and 550 nm (□) plotted against the phase δ derived with the new method. $|\sin\delta|$ is represented by straight lines. It is obvious that the difference of $|\sin\delta|$ for 540 nm and 550 nm increases together with the phase δ as a result of the larger thickness L of the wedge.

for the final δ to $m = m' + 1$ and thus the final $\delta = (m' + 1)\pi + \delta_0$ (Fig. 3). A similar analysis can lead to the reassignment of the initially calculated order in the case of a negative slope of $|\sin\delta(k)|$ leading to a final (of either $\delta = (m' + 1)\pi - \delta_0$ or $\delta = m'\ \pi - \delta_0$.

It is worth noticing that in determining the extinction angle, φ, the value of δ either leads to φ being the angle to the fast or to the slow axis, e.g. when the phase δ lies between $(2m-1)\pi$ and $2m\pi$ the φ measured is the angle between the horizontal and the fast axis, instead of the slow axis (Fig. 1b). Determination of the absolute magnitude of δ enables one always to assign the orientation φ with respect to a common axis, which we normally take for convenience to be the slow axis.

3. Experimental

It is obvious from Eq. (13) that the error when calculating δ_1 is inversely proportional to the relative difference between the two wavelengths used for the δ_1 calculations. Thus, the set of wavelengths used for the experiment needs to be chosen with care. The necessary considerations are: (1) over which wavelength interval can it be assumed that the dispersion is negligible? and (2) how big is δ? The wavelengths should be chosen so that Q will not exceed 1.

In practice we have found that a set of interference filters with wavelengths of 550 nm, 580 nm and 600 nm, for which Q does not exceed 1 for $\delta < 40$, is applicable to most

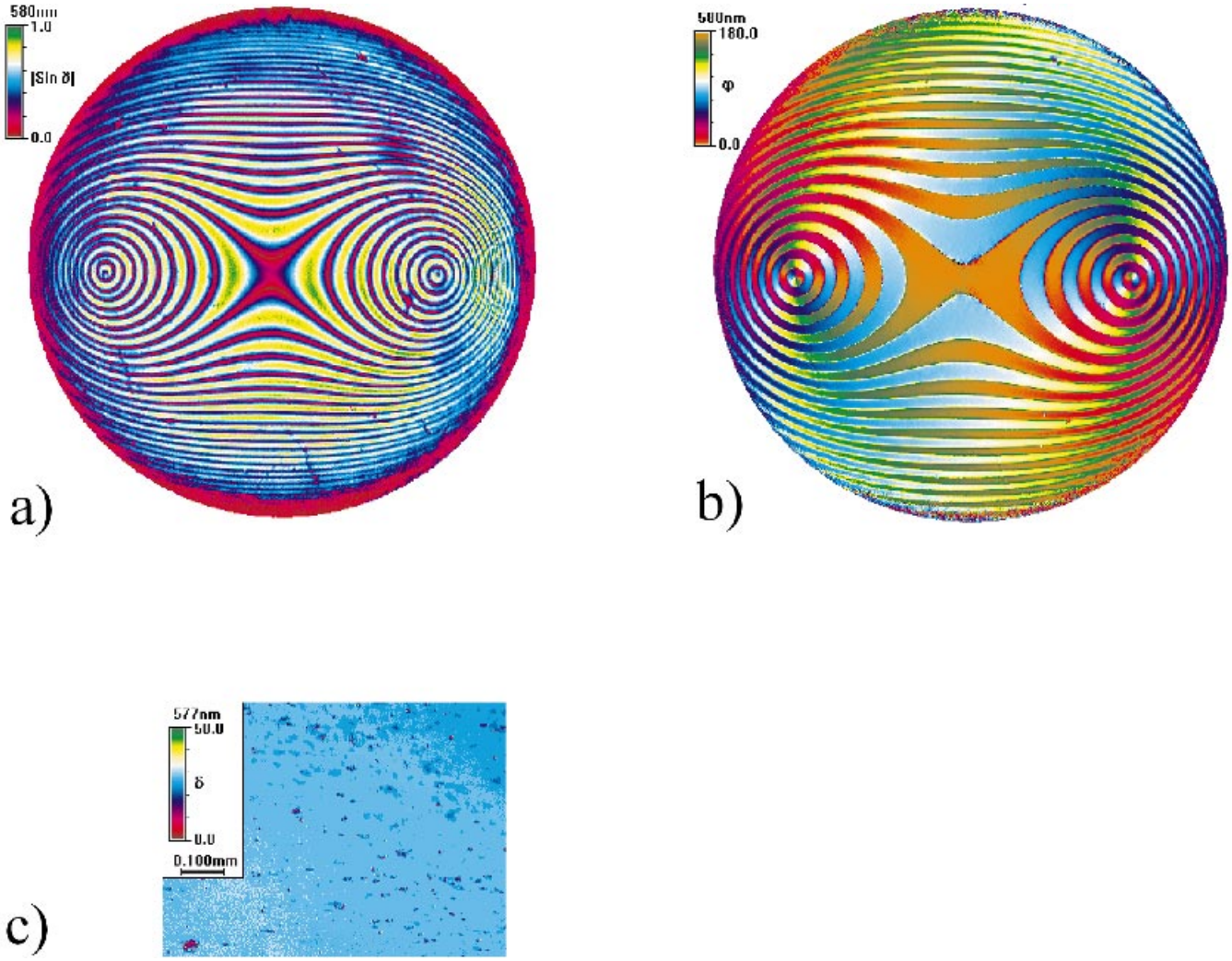

Fig. 5. (a) Conoscopic image of a (010)-cut crystal of mannitol, thickness 0.450 mm. Each red-coloured 'ring' represents values of $|\sin\delta|$ of 0, where m increases by 1. (b) Conoscopic image with respect to the (relative) orientation angle which steps through 90°, when δ lies between $(2m-1)\pi$ and $2m\pi$. (c) Orthoscopic image of the absolute phase along [010] in mannitol. Three interference filters were used: 550 nm, 580 nm and 600 nm with a half-width of 10 nm.

samples. It was even possible to use 540 nm and 550 nm filters in one case due to very little initial error on the $\delta_{0,1}$ and $\delta_{0,2}$, which were averaged over 400 pixels.

The quality of the interference filters was checked by the supplier (Ealing Electro Optics, Inc., Holliston, MA, U.S.A.) and documented with spectra showing the transmission as a function of the wavelength.

3.1. Quartz wedge

The equations were first tested on a quartz wedge, where the phase difference increases with the thickness of the wedge. The contribution due to dispersion of the double refraction is also in proportion to the thickness and is small at lower δ. The values of $|\sin\delta|$ were derived with the RP method as described above (Glazer *et al.*, 1996). The measurements were carried out at 540 nm and 550 nm using interference filters of 10 nm spectral width with a halogen light bulb serving as the light source.

Equation (13) was used to derive the value of the phase assuming that $S_1 = S_2$ and $Q = 0$. Figure 4 shows the result for increasing thickness of the wedge where the procedure is repeated at different positions along the wedge to derive the phase. From 21 measured $|\sin\delta|$-pairs we found one failure in calculating a correct phase, due to the fact that the above assumptions occasionally fail for high δ-values.

3.2. Conoscopic and orthoscopic images

In order to test the upper limitations of our approach, we tried a (010) cut of an optically biaxial material, mannitol, $C_6H_{14}O_6$ (Kaminsky & Glazer, 1997). Figures 5(a) and (b) show the conoscopic images of $|\sin\delta|$ and the relative extinction φ. A conoscopic image arises from the back-focal plane in the microscope and represents an image of the light source; with the sample within the optical train, a variation of the final state of polarization can be seen that depends on the path of the light as it goes through the sample. Each

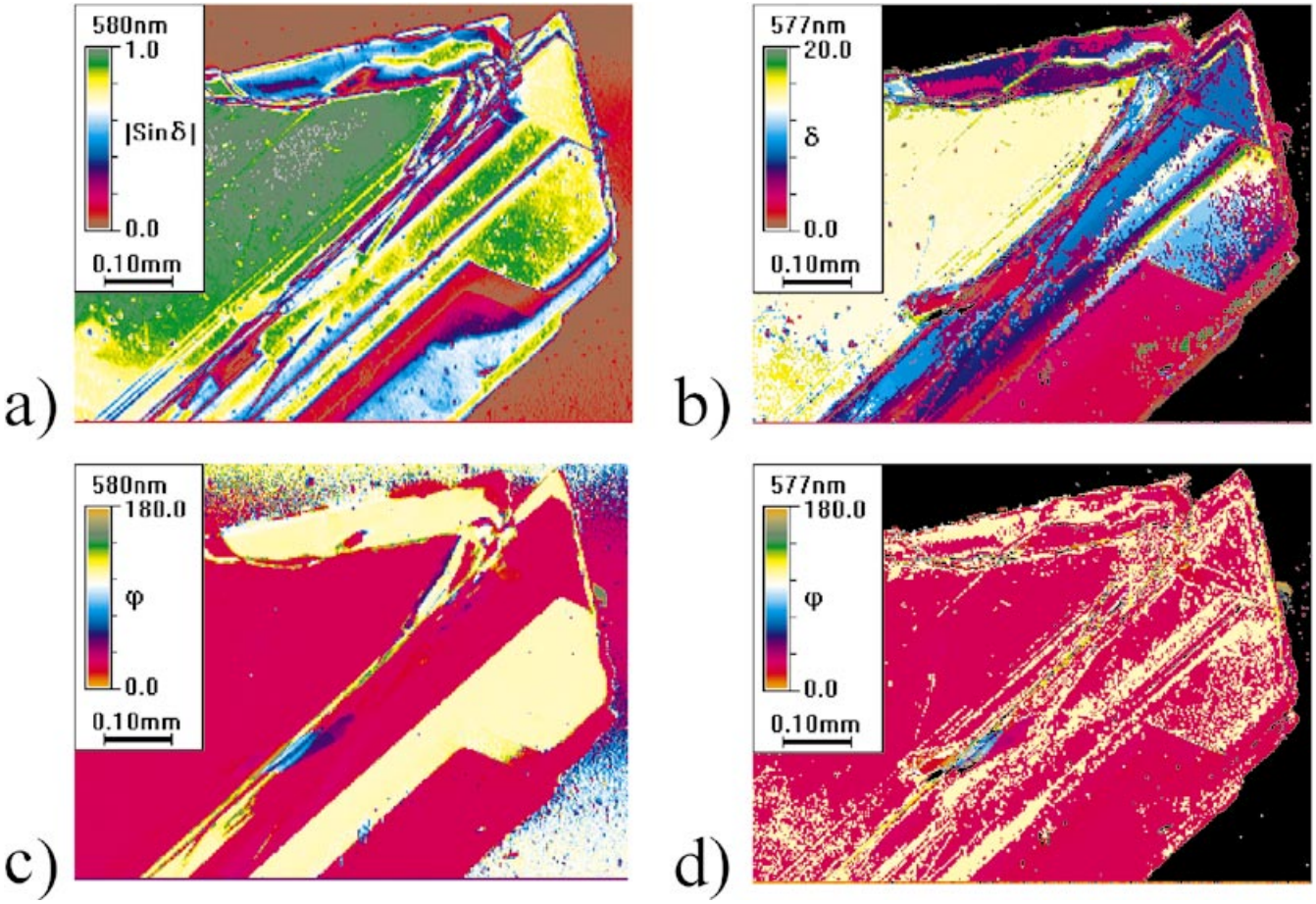

Fig. 6. Gypsum fragment of varying thickness. (a) $|\sin\delta|$, (b) absolute, (c) apparent (when assuming that $m = 0$) orientation of the slow axes at 580 nm, (d) absolute orientation of the slow axis. The wavelengths used to derive the absolute phase and absolute orientation were 550 nm, 580 nm and 600 nm. If for a point in the image $|\sin\delta| < 0.04$ for all three wavelengths, then this point is taken to belong to the background, and is coloured black.

pixel in each image represents a different angle towards the sample normal vector. This angle becomes more obtuse the further a pixel deviates from the centre of the image. As a further result, the orientation of the ellipsoidal section normal to the light path depends on the direction of the light.

The RP method is able to separate out this orientation angle and produce two different conoscopic images, the first depending only on the retardance, the second only on the extinction (Fig. 5b). Those images are otherwise always merged using conventional techniques (for a description of conoscopic images, see Hartshorne & Stuart, 1964), and as far as we know this is the first time that separate conoscopic images illustrating magnitude and orientation have been demonstrated. We see further that the apparent extinction angle exhibits changes by 90° when passing through a retardance of $m\pi$ (change in colour from blue to orange in Fig. 5). The images allow one to count the order $2m$ easily, starting at the two distinct optical axes, where the value of δ equals 0. As a result, one expects a value for δ in the centre of the image of about 28. Figure 5c shows the result when using ordinary, orthoscopic geometry, which gives an image of the crystal itself, and indeed the colour level reveals a δ of about 27.6(3). The interference filters used were of 10 nm spectral half-width at wavelengths of 550 nm, 580 nm and 600 nm.

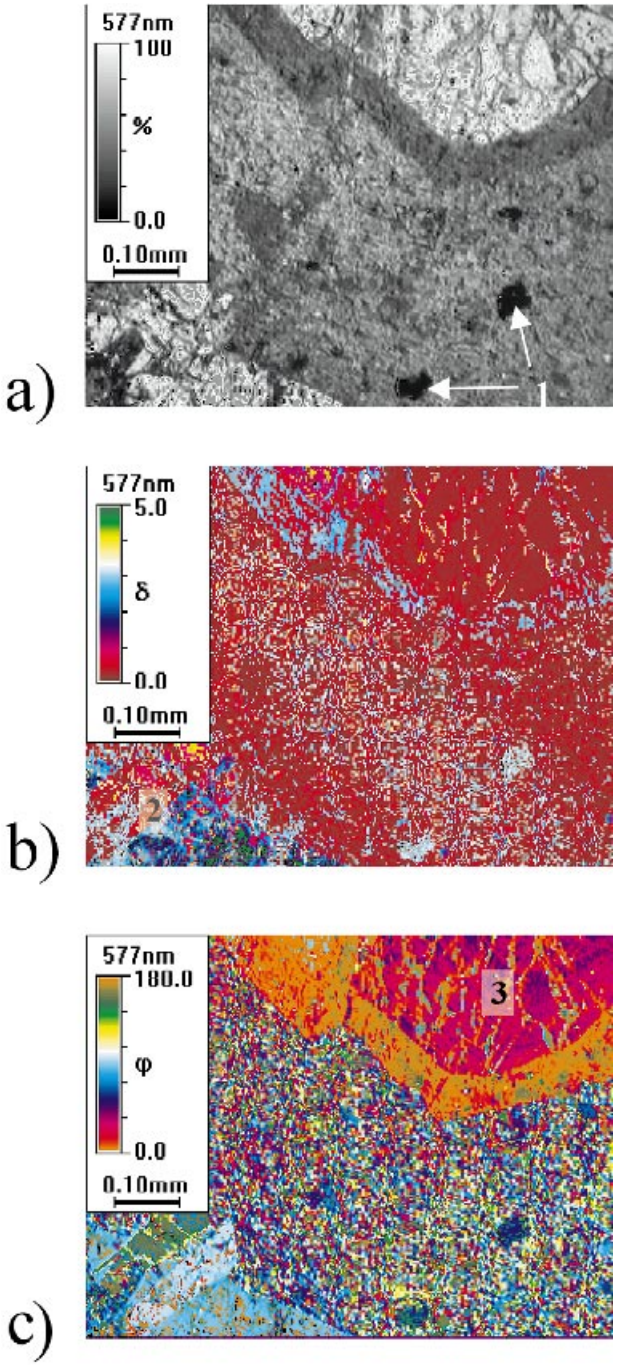

Fig. 7. Andesite, thickness 30 μm. (a) transmittance (black = opaque), (b) absolute phase, (c) absolute orientation of the slow axis. Interference filters as in Fig. 6.

3.3. Gypsum fragment

Gypsum cleaves easily; however, when cut slightly inclined to the easy cleavage plane, the resulting sample exhibits regions of different thickness. As a result, we obtain a coloured $|\sin\delta|$ image (Fig. 6a) in the RP microscope that consists of several orders $2m$ of δ (Fig. 6b) as illustrated by the changes in orientation of the apparent extinction (Fig. 6c). After calculating δ the true orientation of the slow axis proves to be constant throughout most of the sample (Fig. 6d). The same interference filters as for the orthoscopic image of mannitol were used.

Because gypsum is a material with a high optical dispersion we cannot ignore the second term in Eq. (11). Instead, we recast this equation as:

$$\frac{\partial\delta_0}{\partial k} = \pm L\left\{(n_2 - n_1) + k\frac{\partial}{\partial k}(n_2 - n_1)\right\}$$
$$= \pm\delta\left\{\frac{1}{k} + \frac{1}{(n_2 - n_1)}\frac{\partial}{\partial k}(n_2 - n_1)\right\}$$

Leading to:

$$R\delta = \pm k\frac{\partial\delta_0}{\partial k}, \quad \text{where} \quad R = \left\{1 + \frac{k}{(n_2 - n_1)}\frac{\partial}{\partial k}(n_2 - n_1)\right\} \tag{14}$$

R can be calculated if we assume that the orientation of the slow axes of the indicatrix is constant throughout the sample. This enables us to refine the value R in order to achieve a uniform orientation image. In the case of gypsum we find $R = 1.09(1)$ at $\lambda = 580$ nm.

3.4. Rock minerals

As a practical example of the use of the new method, a 30 μm thick cross-section of andesite has been investigated.

We used filters at 550 nm, 580 nm and 600 nm. Figure 7a shows the transmittance I_0 of this rather heterogeneous sample. Nearly black grains of magnetite(1) within the fluxional groundmass can be distinguished from the other more transparent phenocrysts(2,3). On the bottom left (blue) in Fig. 7(b) we see strongly birefringent grains of lamella twinned plagioclase(2). The zoned phenocryst(3) (augite, basal section) in Fig. 7(c) extinguishes symmetrically. The plagioclase extinguishes obliquely as expected.

4. Conclusion

The example of the quartz wedge clearly shows how a change of wavelength can be used to estimate the absolute order of the phase (from experimental $|\sin\delta|$ measurements. The reliability of the method depends on the accuracy in measuring $|\sin\delta|$ and the amount of dispersion of the double refraction. If the latter is known, the method can be applied to even higher values of the order $2m$ than those shown here. It should be pointed out that the method is always able to detect whether the phase, δ, relative to a starting point, increases or decreases due to temperature changes or other external factors.

The method can be applied to phase values up to at least 30 with a reliability of about 5%, as shown in the (010)-cut of mannitol and the gypsum fragment.

If the accuracy in measuring $|\sin\delta|$ can in future be enhanced it will be possible to separate out the dispersion more precisely by comparison of the calculated δ and the measured $|\sin\delta|$ values. This would be in itself rather useful, as the dispersion may be itself characteristic of a particular material, thus helping in the task of identifying a substance automatically.

Finally, the combination of the RP method and a change of wavelength provides the means to measure double refraction of any material without the need for further compensatory steps. The resolution obtained with the SWRP-method, or rather the dynamic range, is increased dramatically. It may now be possible with this technique to derive characteristic fingerprints of materials such as rock-minerals.

Acknowledgements

We thank Oxford Cryosystems, Jesus College Oxford, the Engineering and Physical Sciences Research Council (Great Britain), and the Hougaard & Andreassens Foundation (Denmark) for financial support.

References

Ajovalasit, A., Barone, S. & Petrucci, G. (1995) Towards RGB photoelasticity – full field automated photoelasticity in white light. *Exp. Mechanics*, **35**, 193–200.

Ajovalasit, A., Barone, S. & Petrucci, G. (1998) A review of automated methods for the collection and analysis of photoelastic data. *J. Strain Anal*, **33**, 75–91.

Buckberry, C. & Towers, D. (1996) New approaches to the full-field analysis of photoelastic stress patterns. *Optics Lasers Engineering*, **24**, 415–428.

Glazer, A.M., Lewis, J.G. & Kaminsky, W. (1996) An automatic optical imaging system for birefringent media. *Proc. R. Soc. London Series*, **A452**, 2751–2765.

Greivenkamp, J.E. & Bruning, J.H. (1992) Phase Shifting Interferometry. *Optical Shop Testing*. 2nd edn (ed. by D. Malacara), pp. 501–599. John Wiley & Sons, Inc, New York.

Hartshorne, N.H. & Stuart, A. (1964) *Practical Optical Crystallography*. Edward Arnold, London.

Hecht, E. & Zajac, A. (1974) *Optics*. Addison-Wesley, Reading, Massachusetts.

Hecker, F.W. & Morche, B. (1986) Computer-aided measurement of relative retardations in plane photoelasticity. *Experimental Stress Analysis* (ed. by H. Wieringa), pp. 535–542. Martinus-Nijhoff, The Hague.

Kaminsky, W. & Glazer, A.M. (1997) Crystal optics of D-mannitol, $C_6H_{14}O_6$: crystal growth, structure, basic physical properties, birefringence, optical activity, Faraday effect, electro-optic effects and model calculations. *Z. Kristallogr.* **212**, 283–296.

Moxon, J.R.L. & Renshaw, A.R. (1990) The simultaneous measurement of optical-activity and circular-dichroism in birefringent linearly dichroic crystal sections. 1. Introduction and description of the method. *J. Phys. Condens. Matter*, **2**, 6807–6836.

Redner, A.S. (1985) Photoelastic measurements by means of computer-assisted spectral-contents analysis. *Exp. Mechanics*, **25**, 148–153.

Shurcliff, W.A. (1962) *Polarised Light*. Harvard University Press, Cambridge, Massachusetts and Oxford University Press, London.

Whittaker, P. (1995) Polarised light microscopy in biomedical research. *Microsc. Anal*, **45**, 15–17.

Wood, I.G. & Glazer, A.M. (1980) Ferroelastic phase transition in $BiVO_4$. I. Birefringence measurements using the rotating-analyser method. *J. Appl. Crystallogr.* **13**, 217–223.